Electronic supplementary information (ESI) for manuscript

Electronic structure and magnetic coupling in selenium substituted pyridine-bridged bisdithiazolyl multifunctional molecular materials

Cristina Roncero-Barrero, Jordi Ribas-Arino, Mercè Deumal, and Ibério P. R. Moreira

Departament de Ciència de Materials i Química Física & Institut de Química Teòrica i Computatcional (IQTCUB), Universitat de Barcelona, c/ Martí i Franquès 1-11, 08028 Barcelona, Spain

Section 1. Band gap.

Our results show that the values of the band gaps depend on the magnetic solution, ranging from 1.30-1.45 eV for (S,S), 1.13-1.30 eV for (S,Se), 1.25-1.36 eV for (Se,S), and 1.15-1.24 eV for (Se,Se) (see Table S1). Notice that, in the case of (Se,Se), the values for the low temperature solution are almost the same 1.15-1.25 eV. It can be observed that the value of the band gap follows the same trend as the conductivity values, with larger values corresponding to lower conductivities (see Table S1). Yet the differences among the band gaps are not large enough to explain by themselves the conductivities found experimentally. Interestingly enough, the band gap is sensitive to the magnetic solution and a significant change of 0.15 eV for (S,S) and (S,Se) and 0.11 eV for (Se,S) and (Se,Se) is observed when switching from the FM to the AFM2/AFM3 solutions.

Table S1. Calculated band gaps (in eV) of the FM and different BS solutions (see main text Figure 3 for spin arrangement) for S/Se bisDTA-compounds. The two numbers in the FM solution correspond to the $\alpha - \alpha$ and lowest $\alpha - \beta$ gap (see text). Experimental conductivity is also given.

System	T/K	σ (S·cm^{-1})	FM	AFM	AFM1	AFM2	AFM3	AFM4
(S,S)	100	$3.2\cdot10^{-6}$	2.58/1.30	1.34	1.43	1.45	1.36	1.43
(S,Se)	100	$1.0\cdot10^{-4}$	2.11/1.13	1.15	1.28	1.30	1.31	1.21
(Se,S)	100	$2.2\cdot10^{-5}$	2.17/1.25	1.26	1.35	1.36	1.27	1.37
(Se,Se)	100	$3.0\cdot10^{-4}$	2.08/1.15	1.17	1.24	1.26	1.24	1.22
	2		2.11/1.15	1.18	1.22	1.24	1.25	1.20

Section 2. Charge and spin distribution.

Mulliken charges and spin densities for the lowest energy solution of each material have been analysed since, although it is known they have to be taken cautiously, they can provide interesting qualitative information to rationalise the electron distribution in the materials. Interestingly, analysis of the charge and spin distribution shows that the values are almost independent of the magnetic solution and, hence, the system shows neutral paramagnetic molecular entities with well-defined charge and spin distributions.

Regarding the atomic charges for the lowest energy solution of each material (see Figure S1), it can be observed that the atoms belonging to the central ring have values that are similar for all the systems. However, important differences appear when comparing the atoms in the outer rings. While the N atom has a large negative charge of *ca.* -0.53e$^-$ in all cases, the atoms in E_2 position have positive charges whereas atoms in E_1 positions have negative charges with large differences but showing large variations along the series (see main text Figure 1 for reminder on E_1 and E_2 positions).

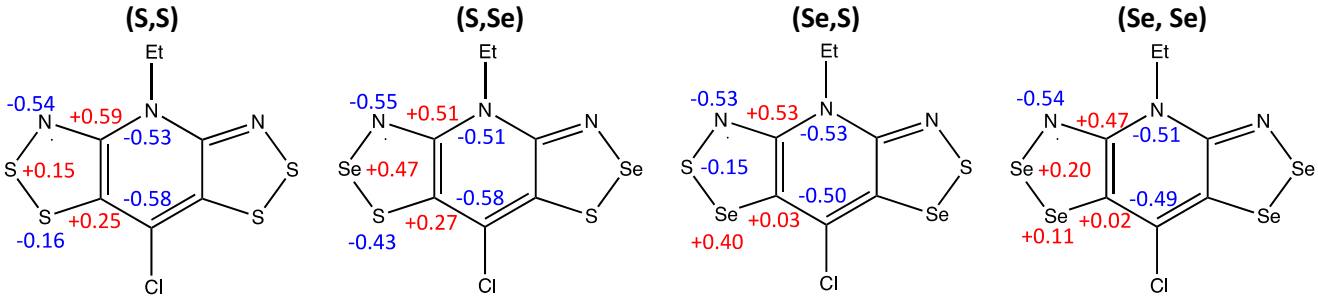

Figure S1: Atomic charges (in electrons) obtained from Mulliken analysis for the AFM solution of the systems. Values for the other electronic solutions show small differences (< 0.02) with respect to the values shown here and represent the same electronic distribution for all the molecular entities.

The spin distribution for all the compounds shows that is almost independent of the particular magnetic solution and, thus, each radical can be considered a local S = 1/2 effective spin particle in order to describe magnetic properties of the systems (see Figure 5 of the main text for (S,S) and (S,Se), and Figure S2 for (Se,S) and (Se,Se)). The population analysis shows that one unpaired electron is delocalised over the π-system of each molecular building block and the atomic spin is larger on N, E_1 heteroatoms, and on the C atom of the central ring connected to Cl. Values for the other electronic solutions show small differences (< 0.03) with respect to the values shown here and correspond to the same spin distribution. It must be stressed that the spin distribution is very similar for all the solutions (see Figure S3 for comparison of FM and some other solutions).

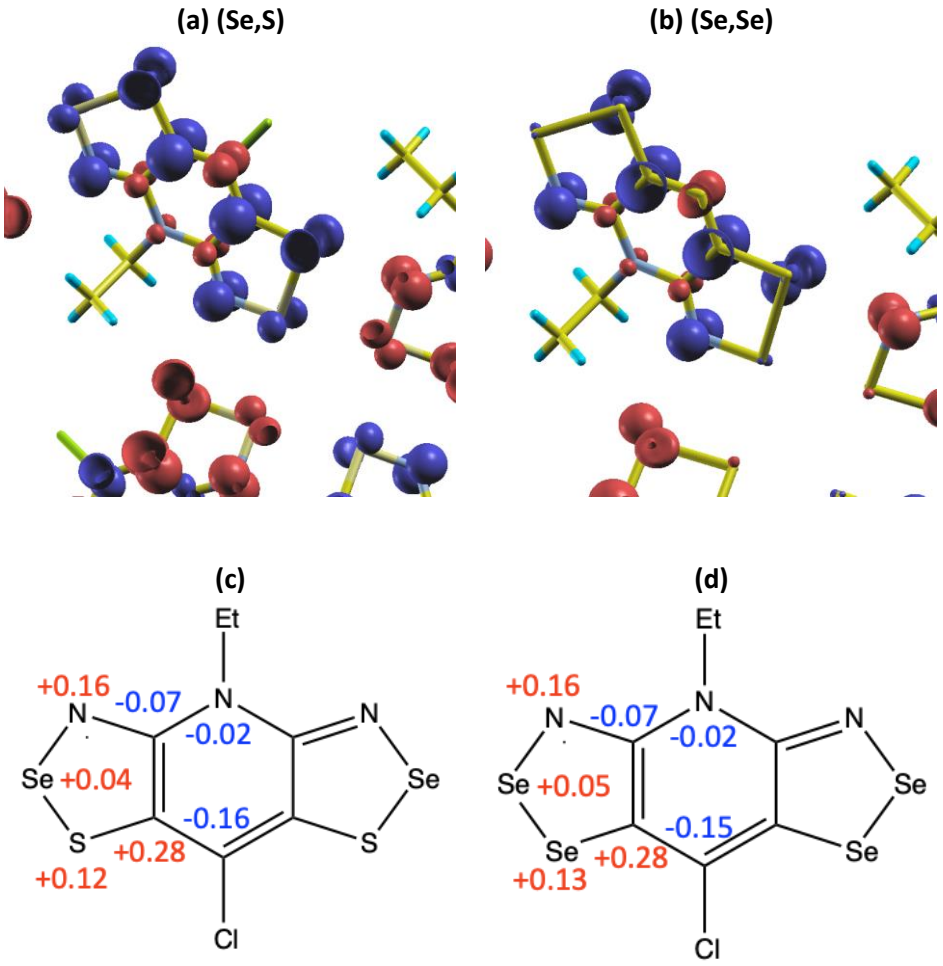

Figure S2: Spin density distribution of the AFM solutions of the (a) (Se,S) and (b) (Se,Se) systems to compare with Figure 5 of the manuscript. Colour code: Alpha and beta spin densities in blue and red, respectively (0.005 a.u. isosurface). Atomic spin densities (in electrons) obtained from Mulliken analysis for the same solutions. Atomic spin densities (in electrons) obtained from Mulliken analysis for the same solutions are reported in (c) and (d).

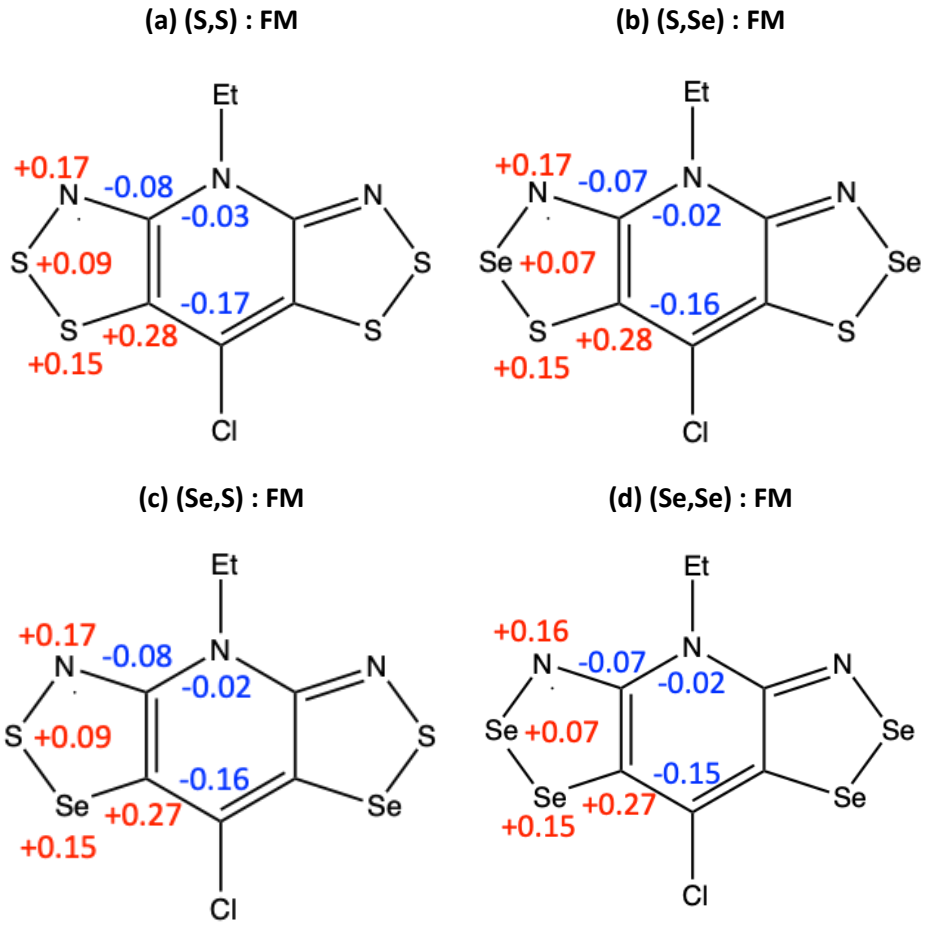

Figure S3: Atomic spin densities (in electrons) obtained from Mulliken analysis for the FM solutions of the (a) (S,S), (b) (S,Se), (c) (Se,S) and (d) (Se,Se) systems to compare with Figure 5 of the manuscript. Colour code: Alpha and beta spin densities in blue and red, respectively. Values for the other electronic solutions show small differences (< 0.03) with respect to the values shown here (for instance, compare with those obtained for AFM in main text Figure 5 and S2).

Table S2 Intermolecular distance analysis (in Å) of the studied magnetic contacts. Distances between molecular mass centroids and the shortest contacts between relevant atomic positions have been listed, as well as the computed exchange couplings (See Figure 7 of the main text for J_{AB} notation).

System		d. cent.	$N_A\cdots N_B$	$N_A\cdots E_{1B}$	$N_A\cdots E_{2B}$	$E_{2A}\cdots E_{2B}$	$E_{2A}\cdots E_{1B}$	J_{AB} /cm^{-1}
(S,S)	**π**	4.03	4.03	3.53	3.76	4.03	3.68	-3.0
	d	11.17	6.54	6.53	5.19	3.90	5.46	-0.5
	ab	8.37	5.71	3.35	4.24	3.49	3.52	1.2
	2c	8.00	4.67	3.53	3.48	3.34	4.30	3.4
(S,Se)	**π**	4.02	4.02	3.55	3.77	4.02	3.74	4.1
	d	11.24	6.68	6.70	5.19	3.76	5.51	-1.4
	ab	8.43	5.83	3.41	4.26	3.40	3.61	3.5
	2c	8.04	4.76	3.56	3.47	3.27	4.40	7.0
(Se,S)	**π**	4.09	4.09	3.58	3.86	4.09	3.68	-3.8
	d	11.34	6.72	6.65	5.32	3.96	5.52	-1.1
	ab	8.13	4.81	3.65	3.63	3.39	4.37	2.5
	2c	8.48	5.79	3.28	4.35	3.55	3.45	2.4
(Se,Se)	**π**	4.13	4.13	3.65	3.91	4.13	3.78	4.1
	d	11.44	6.84	6.83	5.31	3.83	5.61	-1.0
	ab	8.20	4.89	3.70	3.61	3.36	4.53	5.6
	2c	8.56	5.89	3.34	4.34	3.46	3.59	3.6

A preliminary analysis of the intermolecular distances seems to be able to provide the most relevant through space interactions in order to establish the dominant magnetic coupling constants in the materials. However, this by no means provides a simple and univocal assignation since the molecular topology and the possible contacts between neighboring radicals are complex and strongly dependent on the definition of each pair considered. In Table S2 we provide a set of 6 relevant contacts between A and B molecular entities forming a pair to which the J_{AB} interaction can be assigned. The simplest assumption of a given magnetic net by assigning the magnetic moment of a given radical to its centroid of mass is only evident to define the obvious J_{π} interaction. The lateral contacts (both in plane and interplane interactions described in Figure 7) can be rationalized by taking into account the shortest interatomic distances between two atoms belonging to radical A and radical B. In this case, the $N_A\cdots N_B$, $N_A\cdots E_{1B}$, $N_A\cdots E_{2B}$. $E_{2A}\cdots E_{2B}$, and $E_{2A}\cdots E_{1B}$ represent the shortest values observed in the structures. Clearly, the $N_A\cdots E_{1B}$ and $E_{2A}\cdots E_{2B}$ suggest that the set of J_{AB} parameters considered in this work are the most relevant since other possible contacts become significantly distant and the corresponding magnetic couplings are expected to be small. This shows the difficulty in assigning a univocal interaction path and an exhaustive inclusion of other pair interactions becomes cumbersome and, hence, we limit ourselves to the set of J_{AB} couplings considered.

Section 3. Band structure and normalized density of states

Analysis of the band structure and the projected density of states of the ground state solutions for all four materials using X-Ray data at 100 K (namely, AFM2 solution for (S,S), FM for (S,Se) and (Se,Se) and AFM1 for (Se,S), see Figure S4) shows that all the systems are described as magnetic semiconductors with a gap of *ca.* 1.3 eV and similar band structures.

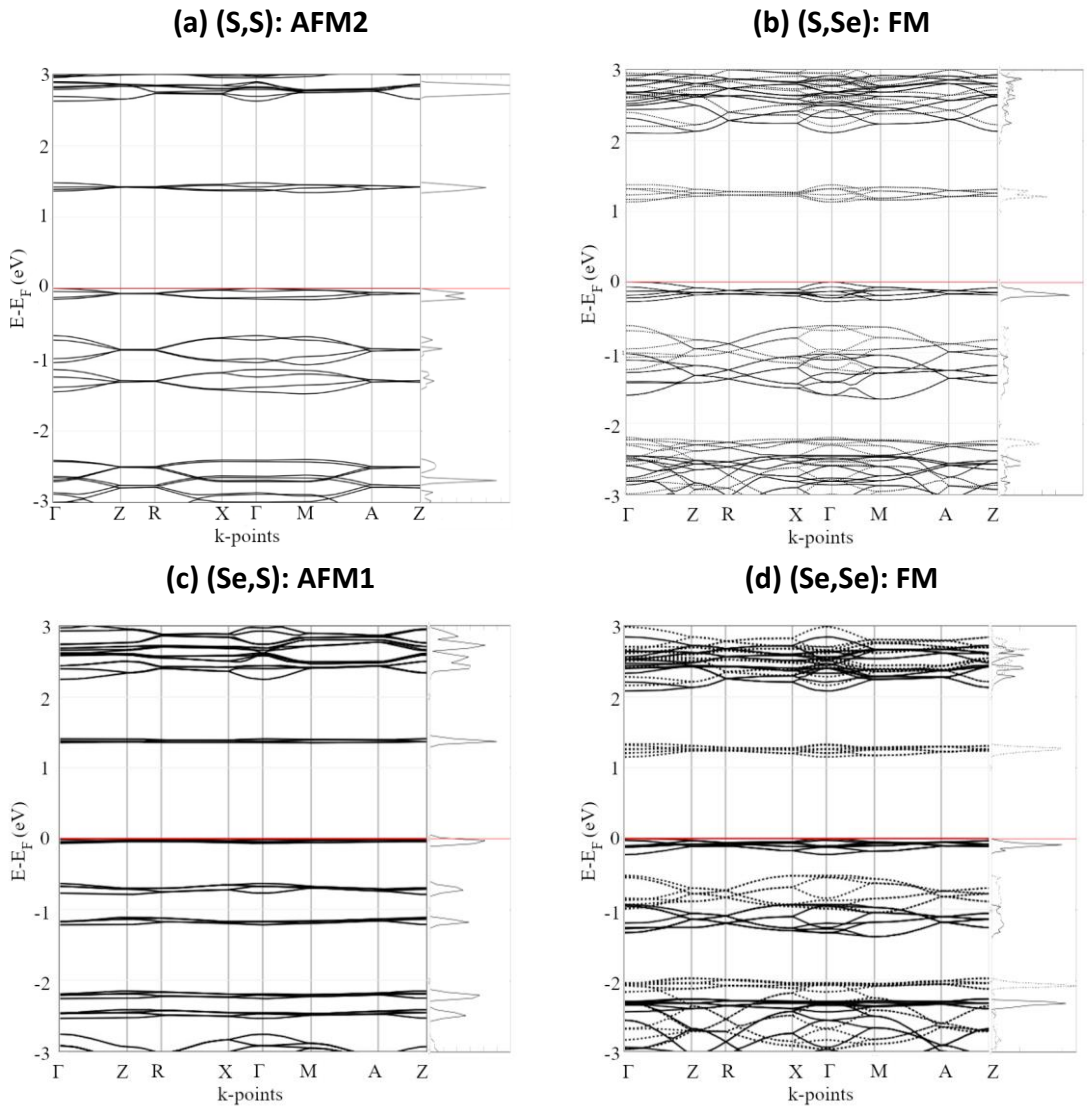

Figure S4. Band structure plots and normalized density of states plots of the ground state solutions for all four bisDTA materials, i.e., AFM2 solution for (S,S), FM for (S,Se) and (Se,Se) and AFM1 for (Se,S) compounds. Note that calculations have been carried out using X-Ray data at 100 K.

The AFM2 spin state has been chosen for comparison purposes across all four isostructural derivatives (see Figure S5). It can be observed that the upper valence bands have a small

dispersion (*ca.* 0.2 eV that is slightly larger for the (S,S) compound) and are dominated by E_1, E_2 and N π-contributions. The conduction band also has a large contribution of these heteroatoms but show more differences in terms of band dispersion: (S,Se) shows a value of 0.25 eV that is significantly larger than the 0.15-0.18 eV values of the remaining systems. As a final comment, the fact that the N-E_1-E_2 heteroatoms have a strong participation in both the valence and the conducting bands defining the insulating state is a clear indication that these atoms will have a decisive contribution in defining the effective conduction paths for electrical conductivity.

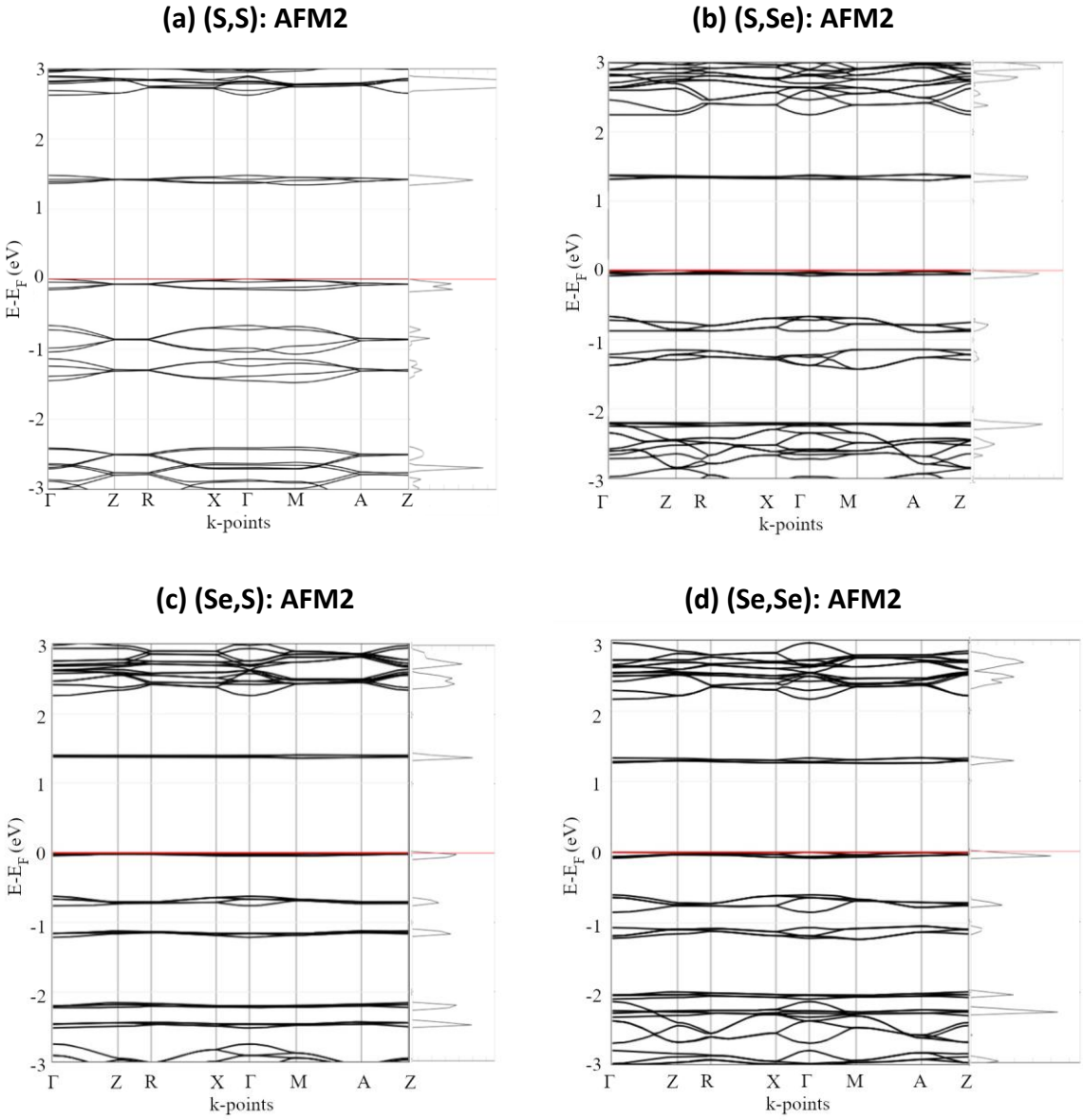

Figure S5. Band structure plots and normalized density of states plots of the AFM2 solution for the studied compounds. The top of the valence bands has been set at 0 eV.

Finally, band structure calculation of FM, AFM1, AFM2, AFM and CS states have been performed on (Se,Se) using a recently characterised X-Ray crystal structure at 2 K (see Figures S6 and S7). Notice that FM and AFM band diagrams reported here have been obtained in a 1x1x2 supercell of the crystallographic cell.

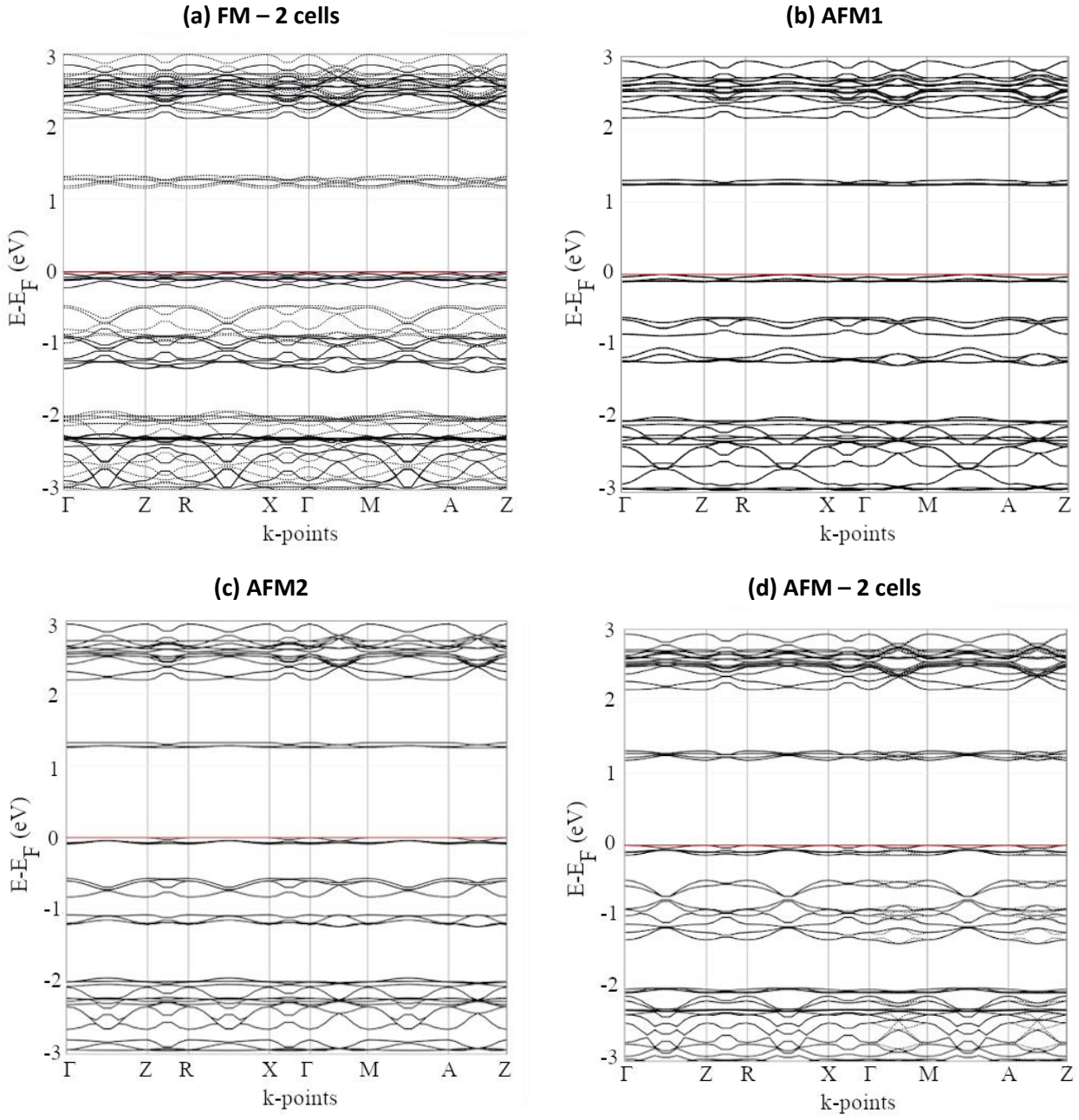

Figure S6. Band structure plots of (Se,Se) compound using X-Ray crystal structure determined at 2K.

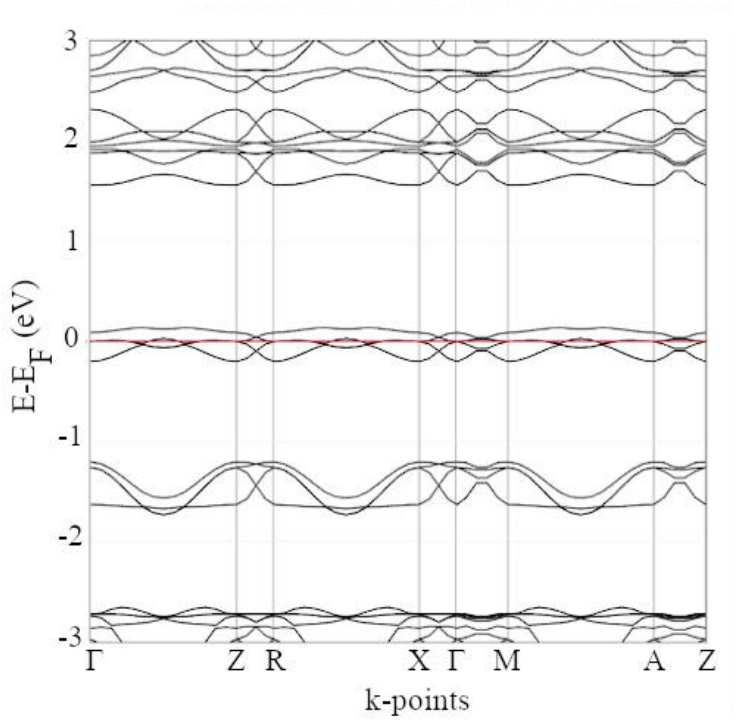

Figure S7. Band structure plot of the CS solution for (Se,Se) compound using X-Ray crystal structure determined at 2 K.